Porous Cage Catenanes | Hot Paper

DOI: 10.1002/anie.201400285

A Shape-Persistent Quadruply Interlocked Giant Cage Catenane with Two Distinct Pores in the Solid State**

*Gang Zhang, Oliver Presly, Fraser White, Iris M. Oppel, and Michael Mastalerz**

Abstract: *Discrete interlocked three-dimensional structures are synthetic targets that are sometimes difficult to obtain with "classical" synthetic approaches, and dynamic covalent chemistry has been shown to be a useful method to form such interlocked structures as thermodynamically stable products. Although interlocked and defined hollow structures are found in nature, for example, in some viruses, similar structures have rarely been synthesized on a molecular level. Shape-persistent interlocked organic cage compounds with dimensions in the nanometer regime are now accessible in high yields during crystallization through the formation of 96 covalent bonds. The interlocked molecules form an unprecedented porous material with intrinsic and extrinsic pores both in the micropore and mesopore regime.*

The synthesis of mechanically interlocked molecules has evolved from being a scientific curiosity to a renowned subtopic in supramolecular chemistry.[1] Interlocked molecules, such as catenanes, rotaxanes, or trefoil knots, are "molecules" by definition because at least one covalent bond has to be broken to decompose two or more molecular parts, which are mechanically interlocked and interact only through noncovalent interactions.[1] After catenanes had been predicted theoretically, their first statistical syntheses suffered from low yields.[2] Later on, Sauvage and co-workers introduced a remarkable synthetic improvement by using metal templates to significantly increase the yields.[3] The groups of Hunter, Vögtle, Leigh as well as Stoddart developed methods that are based on weak supramolecular interactions, for example, hydrogen bonding or π–π stacking, to construct catenanes.[4,5] Even multiple interlocked rings, including olympiadan,[6] were accessible as were sophisticated molecular structures, such as Borromean links.[7] For the synthesis of Borromean links, the dynamic formation of covalent imine bonds and coordinative bonds is crucial to allow the system to self-correct its structure.

The dynamic formation of covalent or coordinative bonds is also the basis of high-yielding cage syntheses, which is reflected by the many one-pot procedures that have been published over the last decades.[8] With this method, coordination cages or covalent organic cages with "giant" dimensions from a molecular perspective have become accessible.[9,10] Depending on the conditions or parameters of the dynamic system, monomeric cages sometimes tend to form interlocked or catenated dimeric structures. Although Fujita and co-workers already described the formation of such an interlocked coordination cage in 1999,[11] reports on interlocked or catenated cages are still very rare.[12,13] For instance, Clever et al. recently described the synthesis of interlocked coordination cages, which, for example, allosterically bind tetrafluoroborate anions or show pronounced stepwise oxidation behavior, which is due to the incorporated phenothiazine subunits.[14] Polymeric structures of catenated coordination cages are less common, but have been observed in the solid state.[15]

In contrast to coordination cages, purely organic cages are still rarer.[8a,16] This is even more true for interlocked structures. To the best of our knowledge, only two examples of interlocked organic cage compounds have been described in the literature. Beer et al. used a sulfate anion to preorganize two molecular subunits before synthetically closing the subunits to cages by copper-catalyzed 1,3-dipolar Huisgen additions to obtain an interlocked cage in 21 % yield.[17] The second example was reported by Cooper et al.: Two [4+6] imine cages formed a triply interlocked dimer during crystallization.[18] The monomeric cage subunits have been described before as one of the first examples of forming permanent porous organic materials in the crystalline state with Brunauer–Emmett–Teller (BET) surface areas of 624 $m^2 g^{-1}$.[19] As the cages are synthesized by the reversible formation of twelve imine bonds, those bonds can be dynamically cleaved and closed in solution. However, under certain conditions (e.g., acetonitrile and trifluoroacetic acid), catenated structures are formed preferably to non-catenated structures. Unfortunately, because of the relative small cavity size of each cage, the catenated dimers are basically nonporous in the solid state.[18]

During our ongoing studies on mesoporous shape-persistent cages by the dynamic formation of boronic esters,[10] we observed the formation of a giant quadruply interlocked cage in a one-pot 96-fold(!) condensation reaction of 40 molecules.

[*] Dr. G. Zhang, Prof. Dr. M. Mastalerz
Organisch-Chemisches Institut
Ruprecht-Karls-Universität Heidelberg
Im Neuenheimer Feld 270, 69120 Heidelberg (Germany)
E-mail: michael.mastalerz@oci.uni-heidelberg.de
Dr. O. Presly, Dr. F. White
Agilent Technologies
Yarnton (UK)
Prof. Dr. I. M. Oppel
Anorganische Chemie, RWTH Aachen
Landoltweg 1, 52056 Aachen (Germany)

[**] We like to thank the German Research Foundation (Deutsche Forschungsgemeinschaft, DFG) and the "Fonds der Chemischen Industrie" (FCI) for generous financial support. G.Z. thanks the Alexander-von-Humboldt foundation for a postdoctoral fellowship. Hendrik Herrmann is acknowledged for collecting PXRD data. We are grateful to Bernd Kohl for TGA measurements.

Supporting information for this article is available on the WWW under http://dx.doi.org/10.1002/anie.201400285.

Recently, we described the synthesis of the giant cage **3a** by a 48-fold condensation reaction of benzene tris(boronic acid) **2** and a triptycene tetraol with two ethyl groups attached to the third aromatic ring of the triptycene scaffold (**1a**; Scheme 1).[10] These molecules (**3a**) form a highly porous material with a BET surface area of 3758 $m^2 g^{-1}$ and pores with diameters of >2 nm.[10] The triptycene precursor and other derivatives with alkyl chains in the 13- and 16-position have to be synthesized in eight consecutive steps from commercially available starting materials. However, if the alkyl chains were placed at the bridgehead positions instead, the triptycene tetraol precursor could be made in just three steps in reasonable time and yield. To study the dependence of the cage formation on the solubilizing side chains, we first synthesized the 9,10-dihexyltriptycene **1b** before investigating the cage formation. Surprisingly, despite the long alkyl chains, we observed a lower solubility for triptycene **1b** than for **1a** under the reaction conditions that are typically used to obtain cage compound **3a**.[10] Nevertheless, we applied the original conditions to the new reactants at a higher dilution and obtained a clear solution after heating for 16 hours at 100 °C. The ^{1}H NMR spectrum showed one clear set of signals and was thus similar to the spectrum of cage **3a**, although some of the peaks were more broadened (see the Supporting Information). By diffusion-ordered NMR spectroscopy (DOSY), exclusively one trace of signals with a diffusion coefficient of 8.71×10^{-11} $m^2 s^{-1}$ was observed, which is related to a solvodynamic radius of 2.03 nm, similar to the expected value for cage **3b** (see the Supporting Information).

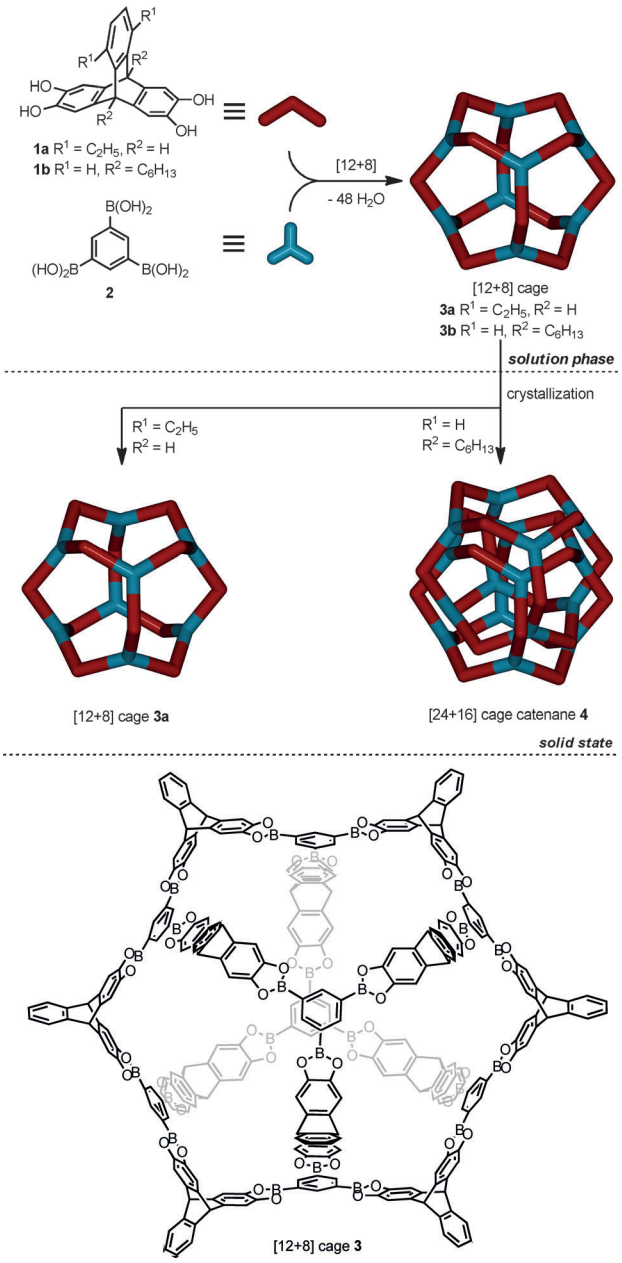

Scheme 1. Top: Synthesis of [12+8] boronic ester cages **3a** and **3b** and formation of the catenated cage **4** during crystallization. Bottom: Molecular structure of one cage; alkyl chains are omitted for clarity.

The compound was crystallized by vapor diffusion of *n*-hexane into a chloroform solution of **3b**, and crystals of sufficient quality for single-crystal X-ray analysis were obtained. To our surprise, we found that two cages **3b** were interlocked in the crystalline state giving catenane **4** (Figure 1) as a racemic crystal with the space group *P*4/*n* (see below). Each catenane **4** consists of two quadruply interlocked cages **3b** (Figure 1a,d). These two interlocked cages show a number of short contacts between the alkyl substituents of one cage molecule and the aromatic planes of the triptycene units of the other cage molecule. It seems that the great number of attractive dispersion interactions is one driving force for catenane formation, resulting in a larger negative enthalpy term for crystal formation. Because of a lack of longer alkyl chains in **3a**, this additional enthalpic contribution by weak dispersion interactions is probably much less pronounced and can be neglected, which explains why **3a** does not form interlocked structures during crystallization.[10] This is in agreement with observations that were made by other groups for similar structures.[11,18,20] However, further derivatives of boronic ester cages have to be made to confirm this hypothesis.

The catenated structure **4** itself is of an ellipsoid shape (Figure 1c), which is open at the two ends. The dimensions of the ellipsoid are approximately 4.6–4.7 nm in length and 4.0 nm in width. As these geometric dimensions do not fit with the measured data from DOSY NMR spectroscopy, it seems to be more likely that the catenane is formed exclusively during crystallization and is transformed into the non-catenated cage **3b** as soon it is redissolved in tetrachloroethane: The ^{1}H NMR spectrum is identical to that of the as-synthesized cage compound **3b**, and no splitting of the signals could be observed, although this is normally the case for catenated cage structures (see the Supporting Information).[11,18,20] Unfortunately, it was not possible to strengthen this hypothesis by mass spectrometry, because even the non-catenated cage **3a** cannot be observed by mass spectrometric methods, which can be explained by the chemical lability of the 24 boronic ester groups. However, from a thermodynamic point of view, it seems to be beneficial that in solution, the entropy increases by unlocking one molecule **4** to give two

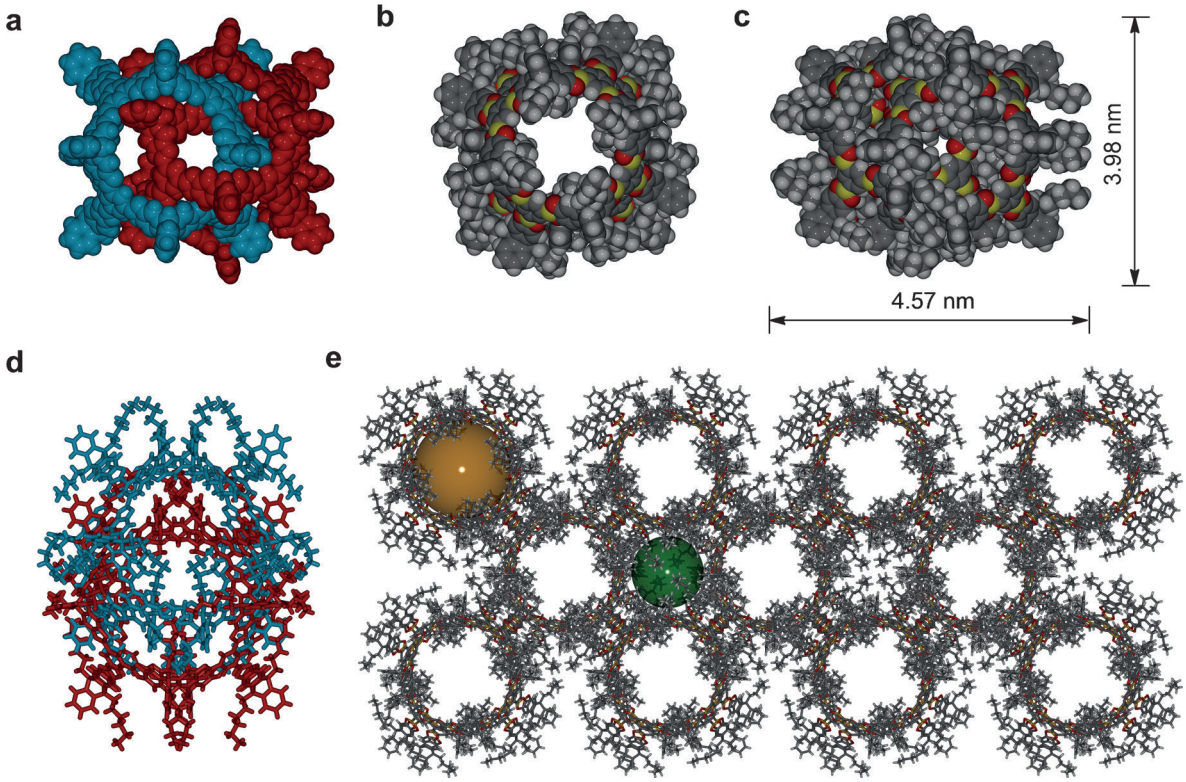

Figure 1. Crystal structure of cage catenane **4**. a) Cage catenane (quadruply interlocked structure) depicted as a space-filling model; alkyl chains are omitted for clarity. The two cages are shown in different colors. b) Cage catenane viewed along the crystallographic *c* axis, depicted as a space-filling model, showing the channel along this axis. Boron red, carbon gray, hydrogen white, oxygen red. c) Cage catenane viewed along the crystallographic *b* axis with molecular dimensions. The cage catenane possesses a nearly closed shell around the central channel. d) Cage catenane represented as a stick model; the alkyl chains are interacting with each other and the aromatic rings of the interlocked other cage. e) Cage catenanes assembled in the solid state, viewed along the crystallographic *c* axis. The orange sphere (2.0 nm) and the green sphere (1.4 nm) show the sizes and positions of the formed channels and pores.

molecules of **3b** and an increase in the overall number of degrees of freedom.

The catenated cage **4** assembles in the crystalline state in a way that two types of pores are inherent in the crystalline state. One is the intrinsic pore of **4**, which accommodates a virtual sphere with a maximum diameter of 2.0 nm; the other one is an extrinsic pore found between the self-assembled cage catenanes. This extrinsic pore accommodates a sphere with a maximum diameter of 1.4 nm (orange and green spheres in Figure 1e). After solvent exchange of inclathrated disordered solvent molecules by immersing the crystals in *n*-pentane (6×12 h)[21] and activating the crystalline compound for nitrogen sorption by evacuating the material at room temperature, we obtained isotherms for **4** that were similar at first glance to those of **3a** (see Figure 2).[10] The isotherm can best be described as a type I isotherm, although it is not as steep as expected for highly microporous organic cage materials in the low-pressure regime.[22] In contrast to the isotherm of **3a**, the isotherm of **4** shows a slightly larger hysteresis. The calculated BET surface area of 1540 $m^2 g^{-1}$ or 1742 $m^2 g^{-1}$ (Langmuir model) is still one of the highest that has been reported for porous organic cage compounds.[22,23] By the formation of catenated dimer **4** through π–π stacking and CH–π interactions, half of the molecular surface of each monomeric cage unit **3b** is already occupied by the stacking interactions that are responsible for the dimerization; therefore, the accessible surface area is roughly halved in comparison to that for the crystals of **3a** (3758 $m^2 g^{-1}$).[10] The pore volume is

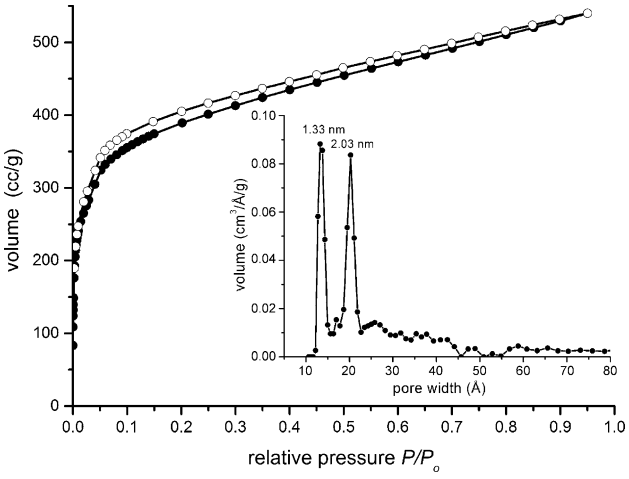

Figure 2. Nitrogen sorption isotherm of crystalline compound **4** after desolvation. Adsorption data points: ●; desorption data points: ○. The inset shows the pore-size distribution by NL-DFT.

0.784 $cm^3 g^{-1}$. By non-local density functional theory (NL-DFT) methods, the pore size distribution was calculated, and two very narrowly distributed, separated peaks with maxima at 1.33 nm and 2.03 nm were obtained (Figure 2, inset). These two peaks fit very well with the two distinct pores (extrinsic and intrinsic) that were found in the crystal structure, which is a hint that the overall crystalline order seems to be intact. Indeed, the pattern obtained by powder X-ray diffraction (PXRD) shows some degree of similarity to a pattern that was simulated from the single-crystal structure of **4** (solvated phase; see the Supporting Information), although it is not the same. Solving three-dimensional structures from PXRD data is not trivial for such large crystalline molecular structures and certainly much more difficult than for crystals of cages of smaller size, for example (for comparison, catenane **4** contains 1008 non-hydrogen atoms, whereas the catenane of Cooper cage CC1 contains only 120 non-hydrogen atoms).[18] However, the NL-DFT data of the two pore sizes would not fit so precisely with those for the crystal structure, if there was not a certain structural similarity of the solvated and desolvated phases. Nevertheless, further investigations to develop a more accurate model of the desolvated phase will be done in due course.

In conclusion, we have shown that the giant shape-persistent cage catenane **4** can be formed in high yields (62 %) by crystallizing the corresponding monomer **3b**. For the formation of **4**, a 96-fold condensation reaction had to occur in one step, which is, to the best of our knowledge, unprecedented for any distinct molecular organic structure. Furthermore, the catenane forms a porous material with a BET surface area of 1540 $m^2 g^{-1}$ with two distinct pores with narrow pore-size distributions with maxima at 1.4 nm and 2.0 nm. Therefore, the material contains one defined micropore and one defined mesopore. This is the first example of a porous molecular catenane. Currently, we are working on getting a deeper insight into the structural needs of the precursor molecules that are necessary to drive the formation of an interlocked structure in the crystalline state. Therefore, the influence of attractive dispersion forces (or CH–π interactions) will be investigated, for example, by using precursors with various alkyl chain lengths.

Experimental Section

For the synthesis and characterization of cage **3b** and cage catenane **4**, see the Supporting Information. Crystals of cage catenane **4** were obtained by vapour diffusion of *n*-hexane into a chloroform solution of **3b.** Crystal structure of **4**: tetragonal, $P4/n$, $a = b = 37.7406(6)$ Å, $c = 47.0432$ (15) Å, $\alpha = \beta = \gamma = 90.0°$, $V = 67006(3)$ $Å^3$, $Z = 8$, $\rho_{calc} = 0.659$ $g\,cm^{-3}$, $\theta_{max} = 40.3420°$, $\lambda(Cu_{K\alpha}) = 1.5418$ Å, $T = 100(2)$ K, 33601 measured reflections, 19063 independent reflections ($R_{int} = 0.0489$), 9562 reflections [$I > 2\sigma(I)$], 736 parameters, $R = 0.1732$, $wR = 0.4856$ (for all data). Data were collected on an Agilent Technologies SuperNova A diffractometer using Cu radiation with an Oxford Cryosystems Cryostream low-temperature device operating at 100 K. Data were processed using the CrysAlisPro software package (Agilent Technologies 2013, CrysAlisPro Software system, version 1.171.36.28, Agilent Technologies UK Ltd, Oxford, UK), solved with SUPERFLIP, and refined using SHELX and the OLEX2 refinement programs.[24] The SQUEEZE function of PLATON was used to remove the electron density of the solvate molecules.[25] Furthermore, it was necessary to use constraints to control the geometry of the aromatic rings and restraints to enforce chemically sensible bond lengths and angles in the hexyl chains. Vibrational restraints were also used to control atomic displacement parameters of various atoms, in particular those in the hexyl chains, which have considerably greater freedom of movement than the main framework. CCDC 980837 contains the supplementary crystallographic data for this paper. These data can be obtained free of charge from The Cambridge Crystallographic Data Centre via www.ccdc.cam.ac.uk/data_request/cif.

Received: January 10, 2014
Revised: February 25, 2014
Published online: April 6, 2014

Keywords: boronic acids · catenanes · dynamic covalent chemistry · porosity · triptycene

[1] For reviews, see: a) G. Barin, R. S. Forgan, J. F. Stoddart, *Proc. R. Soc. London Ser. A* **2012**, *468*, 2849 – 2880; b) R. S. Forgan, J.-P. Sauvage, J. F. Stoddart, *Chem. Rev.* **2011**, *111*, 5434 – 5464; c) J. E. Beves, B. A. Blight, C. J. Campbell, D. A. Leigh, R. T. McBurney, *Angew. Chem.* **2011**, *123*, 9428 – 9499; *Angew. Chem. Int. Ed.* **2011**, *50*, 9260 – 9327.

[2] E. Wasserman, *J. Am. Chem. Soc.* **1960**, *82*, 4433 – 4434.

[3] C. Dietrich-Buchecker, J.-P. Sauvage, J.-P. Kintzinger, *Tetrahedron Lett.* **1983**, *24*, 5095 – 5098.

[4] a) C. A. Hunter, *J. Am. Chem. Soc.* **1992**, *114*, 5303 – 5311; b) F. Vögtle, S. Meier, R. Hoss, *Angew. Chem.* **1992**, *104*, 1628 – 1631; *Angew. Chem. Int. Ed. Engl.* **1992**, *31*, 1619 – 1622; c) A. G. Johnston, D. A. Leigh, R. J. Pritchard, M. D. Deegan, *Angew. Chem.* **1995**, *107*, 1324 – 1327; *Angew. Chem. Int. Ed. Engl.* **1995**, *34*, 1209 – 1212; d) A. G. Johnston, D. A. Leigh, A. Murphy, J. P. Smart, M. D. Deegan, *J. Am. Chem. Soc.* **1996**, *118*, 10662 – 10663.

[5] P. R. Ashton, T. T. Goodnow, A. E. Kaifer, M. V. Reddington, A. M. Z. Slawin, N. Spencer, J. F. Stoddart, C. Vincent, D. J. Williams, *Angew. Chem.* **1989**, *101*, 1404 – 1408; *Angew. Chem. Int. Ed. Engl.* **1989**, *28*, 1396 – 1399.

[6] D. B. Amabilino, P. R. Ashton, A. S. Reder, N. Spencer, J. F. Stoddart, *Angew. Chem.* **1994**, *106*, 1316 – 1319; *Angew. Chem. Int. Ed. Engl.* **1994**, *33*, 1286 – 1290.

[7] a) K. S. Chichak, S. J. Cantrill, A. R. Pease, S.-H. Chiu, G. W. V. Cave, J. L. Atwood, J. F. Stoddart, *Science* **2004**, *304*, 1308 – 1312; b) C. D. Pentecost, K. S. Chichak, A. J. Peters, G. W. V. Cave, S. J. Cantrill, J. F. Stoddart, *Angew. Chem.* **2007**, *119*, 222 – 226; *Angew. Chem. Int. Ed.* **2007**, *46*, 218 – 222; c) C. D. Meyer, C. S. Joiner, J. F. Stoddart, *Chem. Soc. Rev.* **2007**, *36*, 1705 – 1723.

[8] a) G. Zhang, M. Mastalerz, *Chem. Soc. Rev.* **2014**, *43*, 1934 – 1947; b) K. Harris, D. Fujita, M. Fujita, *Chem. Commun.* **2013**, *49*, 6703 – 6712; c) R. Chakrabarty, P. S. Mukherjee, P. J. Stang, *Chem. Rev.* **2011**, *111*, 6810 – 6918; d) M. M. J. Smulders, I. A. Riddell, C. Browne, J. R. Nitschke, *Chem. Soc. Rev.* **2013**, *42*, 1728 – 1754.

[9] Q. F. Sun, J. Iwasa, D. Ogawa, Y. Ishido, S. Sato, T. Ozeki, Y. Sei, K. Yamaguchi, M. Fujita, *Science* **2010**, *328*, 1144 – 1147.

[10] G. Zhang, O. Presly, F. White, I. M. Oppel, M. Mastalerz, *Angew. Chem.* **2014**, *126*, 1542 – 1546; *Angew. Chem. Int. Ed.* **2014**, *53*, 1516 – 1520.

[11] M. Fujita, N. Fujita, K. Ogura, K. Yamaguchi, *Nature* **1999**, *400*, 52 – 55.

[12] a) A. Westcott, J. Fisher, L. P. Harding, P. Rizkallah, M. J. Hardie, *J. Am. Chem. Soc.* **2008**, *130*, 2950 – 2951; b) M. Fukuda, R. Sekiya, R. Kuroda, *Angew. Chem.* **2008**, *120*, 718 – 722; *Angew. Chem. Int. Ed.* **2008**, *47*, 706 – 710; c) R. Sekiya, M. Fukuda, R. Kuroda, *J. Am. Chem. Soc.* **2012**, *134*, 10987 – 10997.

[13] D. M. Engelhard, S. Freye, K. Grohe, M. John, G. H. Clever, *Angew. Chem.* **2012**, *124*, 4828 – 4832; *Angew. Chem. Int. Ed.* **2012**, *51*, 4747 – 4750.
[14] a) S. Freye, J. Hey, A. Torras-Galan, D. Stalke, R. Herbst-Irmer, M. Jihn, G. H. Clever, *Angew. Chem.* **2012**, *124*, 2233 – 2237; *Angew. Chem. Int. Ed.* **2012**, *51*, 2191 – 2194; b) M. Frank, J. Hey, I. Balcioglu, Y.-S. Chen, D. Stalke, T. Suenobu, S. Fukuzumi, H. Frauendorf, G. H. Clever, *Angew. Chem.* **2013**, *125*, 10288 – 10293; *Angew. Chem. Int. Ed.* **2013**, *52*, 10102 – 10106.
[15] a) X. Kuang, X. Wu, R. Yu, J. P. Donahue, J. Huang, C.-Z. Lu, *Nat. Chem.* **2010**, *2*, 461 – 465; b) J. Heine, J. Schmedt auf der Günne, S. Dehnen, *J. Am. Chem. Soc.* **2011**, *133*, 10018 – 10021.
[16] a) M. Mastalerz, *Angew. Chem.* **2010**, *122*, 5164 – 5175; *Angew. Chem. Int. Ed.* **2010**, *49*, 5042 – 5053; b) M. Mastalerz, *Synlett* **2013**, *24*, 781 – 786; c) N. M. Rue, J. Sun, R. Warmuth, *Isr. J. Chem.* **2011**, *51*, 743 – 768, and references therein.
[17] Y. Li, K. M. Mullen, T. D. W. Claridge, P. J. Costa, V. Felix, P. D. Beer, *Chem. Commun.* **2009**, 7134 – 7136.
[18] T. Hasell, X. Wu, J. T. A. Jones, J. Bacsa, A. Steiner, T. Mitra, A. Trewin, D. J. Adams, A. I. Cooper, *Nat. Chem.* **2010**, *2*, 750 – 755.
[19] T. Tozawa, J. T. A. Jones, S. I. Swamy, S. Jiang, D. J. Adams, S. Shakespeare, R. Clowes, D. Bradshaw, T. Hasell, S. Y. Chong, C. Tang, S. Thompson, J. Parker, A. Trewin, J. Bacsa, A. M. Z. Slawin, A. Steiner, A. I. Cooper, *Nat. Mater.* **2009**, *8*, 973 – 978.
[20] N. Ponnuswamy, F. B. L. Cougon, J. M. Clough, G. D. Pantos, J. K. M. Sanders, *Science* **2012**, *338*, 783 – 785.
[21] M. Mastalerz, I. M. Oppel, *Angew. Chem.* **2012**, *124*, 5345 – 5348; *Angew. Chem. Int. Ed.* **2012**, *51*, 5252 – 5255.
[22] a) M. Mastalerz, M. W. Schneider, I. M. Oppel, O. Presly, *Angew. Chem.* **2011**, *123*, 1078 – 1083; *Angew. Chem. Int. Ed.* **2011**, *50*, 1046 – 1051; b) M. W. Schneider, I. M. Oppel, H. Ott, L. G. Lechner, H.-J. S. Hauswald, R. Stoll, M. Mastalerz, *Chem. Eur. J.* **2012**, *18*, 836 – 847; c) M. W. Schneider, I. M. Oppel, A. Griffin, M. Mastalerz, *Angew. Chem.* **2013**, *125*, 3699 – 3703; *Angew. Chem. Int. Ed.* **2013**, *52*, 3611 – 3615; d) J. T. A. Jones, T. Hasell, X. Wu, J. Bacsa, K. E. Jelfs, M. Schmidtmann, S. Y. Chong, D. J. Adams, A. Trewin, F. Schiffman, F. Cora, B. Slater, A. Steiner, G. M. Day, A. I. Cooper, *Nature* **2011**, *474*, 367 – 371; e) T. Hasell, S. Y. Chong, K. E. Jelfs, D. J. Adams, A. I. Cooper, *J. Am. Chem. Soc.* **2012**, *134*, 588 – 598.
[23] M. Mastalerz, *Chem. Eur. J.* **2012**, *18*, 10082 – 10091.
[24] a) L. Palatinus, G. Chapuis, *J. Appl. Crystallogr.* **2007**, *40*, 786 – 790; b) G. M. Sheldrick, *Acta Crystallogr. Sect. A* **2008**, *64*, 112 – 122; c) O. V. Dolomanov, L. J. Bourhis, R. J. Gildea, J. A. K. Howard, H. Puschmann, *J. Appl. Crystallogr.* **2009**, *42*, 339 – 341.
[25] a) P. Van der Sluis, A. L. Spek, *Acta Crystallogr. Sect. A* **1990**, *46*, 194 – 201; b) A. L. Spek, *Acta Crystallogr. Sect. D* **2009**, *65*, 148 – 155.

